

Acoustic emission in the fcc-fct martensitic transition of Fe_{68.8}Pd_{31.2}

Erell Bonnot, Lluís Mañosa, Antoni Planes, Daniel Soto-Parra, and Eduard Vives
*Departament d'Estructura i Constituents de la Matèria, Facultat de Física, Universitat de Barcelona, Martí i Franquès 1,
 08028 Barcelona, Catalonia, Spain*

Benno Ludwig and Christian Strothkaemper
II. Physikalisches Institut, RWTH Aachen University, D-52056 Aachen, Germany

Takashi Fukuda and Tomoyuki Kakeshita
Department of Materials Science and Engineering, Graduate School of Engineering, Osaka University, Suita, Osaka 565-0871, Japan
 (Received 31 July 2008; revised manuscript received 6 October 2008; published 4 November 2008)

An experimental study of acoustic emission (AE) in a single crystal and in a polycrystalline sample of Fe_{68.8}Pd_{31.2} is presented. The samples are studied in a temperature range that is known to include not only a martensitic transition (MT) but also premartensitic effects and strong lattice-parameter variations below the transition. AE activity is compared to calorimetric and magnetic-susceptibility measurements. AE has only been detected during the martensitic transition. The kinetics of the MT for the single crystal exhibits a series of reproducible peaks of activity. This structured activity is not observed for the polycrystal, which shows a single-peak behavior. Despite these differences the AE measurements reveal that the martensitic transitions in both samples start at the same temperature. Results are also compatible with a negligible hysteresis at the transition. The statistics of the amplitude, energy, and duration of AE signals is analyzed in detail and characterized by power-law exponents. For the single crystal the exponents are coincident for heating and cooling ramps and are independent of the rate. For the polycrystalline sample, the exponents are different for heating and cooling.

DOI: [10.1103/PhysRevB.78.184103](https://doi.org/10.1103/PhysRevB.78.184103)

PACS number(s): 81.30.Kf, 43.90.+v, 64.60.av

I. INTRODUCTION

Acoustic emission (AE) detection¹ is a powerful experimental technique for the study of phase transitions in multi-ferroic materials in which the order parameter either is the strain or is coupled to the elastic degrees of freedom. Nucleation of new phases and propagation of interfaces are known to produce transient elastic waves that travel through the sample and that can be detected at its surface by means of suitable transducers. After appropriate analysis of the detected AE signals, relevant information on the transition dynamics can be obtained. Owing to its displacive nature, martensitic transitions turn out to be good examples of transitions giving rise to intense AE. In this paper we focus on the study of AE in a Fe-Pd ferromagnetic shape-memory alloy. From a theoretical point of view, Fe-Pd has been a prototypical material for the study of martensitic phase transitions, and has received a lot of modeling work.² This is because (i) it displays a relatively simple symmetry relation between the parent and the product phases compared to other martensitic transitions and (ii) it shows a rich pretransitional behavior.

A number of interesting phenomena have been found in Fe-Pd alloys by using different experimental techniques. Our aim is to analyze which of the already reported effects generates AE events and to characterize their statistical properties. For Pd contents above 30%, the martensitic transition takes place on cooling from a face-centered-cubic to a face-centered-tetragonal (fct) phase.³ In the absence of a magnetic field and an applied stress, the low-temperature phase exhibits three different equivalent variants, which results in the existence of a complex microstructure.

Measurements of the lattice parameters' dependence on temperature^{3,4} reveal that the transition is first order, spreading over a temperature range of ~ 25 K within which there is a coexistence of the x-ray peaks of the two phases. Moreover, for temperatures well below this coexistence region, the *a* and *c* lattice parameters of the tetragonal lattice exhibit a remarkable monotonous increase on cooling. This effect extends for more than 75–100 K. In particular for an alloy with composition very close to the one studied here, this monotonous increase has been found to be nonlinear and similar to the increase expected for a second-order-like behavior.⁵ Actually, in previous works the transition was classified as nearly second order,³ also because of its small latent heat compared to that of other shape-memory alloys. Moreover, many experimental studies on this alloy (electron microscopy,⁶ standard x ray,⁷ synchrotron radiation,⁴ and neutron diffraction⁷) have been devoted to the study of premartensitic effects (tweed, mixed tetragonal phases, etc.). In some cases premartensitic phenomena have been reported at more than 100 K above the transition temperature.

There is a lot of previous work devoted to the study of the AE during the martensitic transition in a number of alloys. For instance, in Cu-based alloys the martensitic transition is significantly first order and, thus, the AE activity is very high and a large number of signals is easy to record and analyze.^{8–10} The technique has also been applied to the study of the martensitic transition in Ni-Mn-Ga alloys,^{11,12} Ti-Ni alloys,¹³ Fe-Ni alloys,¹⁴ steels,¹⁵ etc. For Fe-Pd alloys, to our knowledge, no AE experiments have been reported until now.

In many cases thermoelastic martensitic transitions are known to proceed by an avalanche dynamics in which, when

cooling or heating at a constant rate, fast events associated with internal displacements of interfaces are separated by much longer periods of inactivity. These AE events (which we will call hits) are defined by appropriate thresholds and can be characterized by their amplitude A , duration Δt , or energy E . The statistics of these properties has been used to classify the transitions into universality classes.¹⁶ Moreover some alloys display an athermal behavior in which the avalanche phenomenon is very reproducible from cycle to cycle. The acoustic activity, therefore, exhibits scaling properties.¹⁷ When the systems are not completely athermal, the study of the rate dependence of the AE allows quantification of the degree of athermality.^{17,18}

The paper is organized as follows: in Sec. II we present the details of the two studied samples and the different experimental setups. In Sec. III we report on the results obtained by AE, calorimetry, and magnetic-susceptibility measurements. In Sec. IV we present the statistical analysis of the AE signals as well as the computation of the exponents characterizing them. Finally in Sec. V we summarize and conclude.

II. EXPERIMENTAL

Two samples with the same nominal composition $\text{Fe}_{68.8}\text{Pd}_{31.2}$ have been studied. The first sample is a single crystal with dimensions of $3.098 \times 2.966 \times 1.138$ mm³ and mass of 0.088 160 g. It was cut from an ingot grown by a floating-zone method, and homogenized in vacuum. After cutting the sample it was further homogenized at 1373 K for 1 h and quenched into a mixture of ice and water in order to eliminate possible remanent deformations. Sample faces are parallel to (100) planes. The second sample is a polycrystal with dimensions of $3.14 \times 2.95 \times 1.09$ mm³ and mass of 0.086 550 8 g. The average grain size, determined by optical microscopy, is ~ 200 μm .

AE was detected using a piezoelectric transducer, acoustically coupled to the sample. The detected signal was preamplified (60 dB) and monitored by an acquisition system from Euro Physical Acoustics S.A., at a sampling rate of 10 Msamples/s. A 100 kHz–1 MHz bandwidth filter was used in order to reduce noise. From the recorded signal, individual AE hits were defined by using a threshold of 22 dB. When the signal crosses the threshold, a hit starts. When the signal remains below the threshold more than $\text{HDT}=30$ μs , the hit ends. The system allows a maximum duration of the detected signals of 10 ms.

Hits were recorded during cooling and heating ramps between 265 and 200 K at rates varying between 0.1 and 10 K/min. The typical number of detected events in a ramp was $\sim 10^4$. In most cases averages over ~ 20 ramps under the same conditions were performed in order to improve the statistics. Runs performed using a dummy sample enabled us to locate the typical noise threshold at 4–5 hits/K at 1 K/min and 10–15 hits/K at 0.1 K/min. Hits are characterized by their amplitude (measured in dB) and duration. Moreover, it should be mentioned that this experimental setup allows the direct measurement of the energy associated with each individual hit by performing a fast integration of the square of

the signal (in volts). The integral is converted to energy (given in aJ) by dividing by a reference resistance of 10 k Ω . This measurement provides information related to the shape of the recorded signals, but its relation to the energy released by the source of AE is not well established.

Two kinds of quantitative data will be presented. On one hand we will show activity plots which display the number of AE events per temperature interval (typically 0.2 K). On the other hand we will study the statistical distribution of the amplitude A and energy E of the individual events. These distributions will be plotted as histograms on log-log plots. As will be seen they can be well fitted by the power laws $p(A) \sim A^{-\alpha}$ and $p(E) \sim E^{-\epsilon}$. The exponents characterizing these laws have been obtained by the maximum-likelihood method,¹⁹ which is independent of the histogram representation (bins, logarithmic scales, etc.).

Transition temperatures in Fe-Pd alloys are known to be very sensitive to composition. In order to compare with AE measurements, we have also performed calorimetry and magnetic-susceptibility measurements. We have used a commercial differential scanning calorimetry (DSC) calorimeter from TA Instruments (MDSC2920). Typical heating and cooling rates were about 5 K/min. Magnetic susceptibility has been measured by using a commercial ac susceptometer (Lakeshore 7000).

III. RESULTS

Figure 1 shows the calorimetric curves corresponding to heating and cooling ramps for the polycrystal and single crystal. Although the calorimetric signal is not very high compared to the base line, it is possible to obtain some quantitative data from the numerical analysis. The starting and final temperatures of the transition can be measured by integrating the signal and obtaining the transformed fraction as a function of temperature. A standard procedure is then to define the starting transition temperature on cooling M_s as the temperature at which the transformed fraction reaches 10% and the finishing transition temperature M_f as the temperature at which the transformed fraction reaches 90%. Similarly, temperatures A_s and A_f are defined on heating.

For the single crystal we have found that the transition extends from $M_s=238$ K to $M_f=210$ K on cooling and from $A_s=210$ K to $A_f=241$ K on heating. The corresponding temperatures for the polycrystal are $M_s=222$ K, $M_f=204$ K, $A_s=210$ K, and $A_f=224$ K. These temperatures are in good agreement with the value $M_s=230$ K reported for an alloy with almost identical composition^{4,5} and also with a linear extrapolation on the phase diagram shown in Ref. 3. Note that calorimetric data suggest that the polycrystal transforms more than 15 K below the single crystal and that for the two samples hysteresis is lower than 2–3 K (obtained from the difference between M_s and A_f).

By numerical integration we can also obtain the values of the latent heat and entropy change. Data are shown in Table I. Values for heating and cooling ramps are coincident within errors. For the sake of comparison we include the data corresponding to a $\text{Fe}_{70.4}\text{Pd}_{29.6}$ sample reported in Ref. 3. The difference in Pd composition may explain the significant difference.

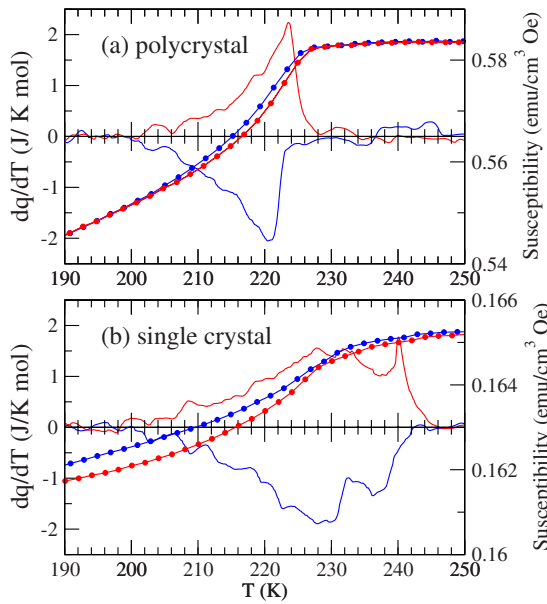


FIG. 1. (Color online) Typical examples of calorimetric curve and magnetic susceptibility (with circles) for (a) the polycrystal and (b) the single crystal. Positive values correspond to a heating ramp (endothermic) and negative values to a cooling ramp (exothermic). For the single crystal magnetic susceptibility has been measured along the [100] direction.

Figure 1 also shows the behavior of the magnetic susceptibility versus temperature. Already from the beginning of the transition (as detected by the calorimetric curves), a change in the susceptibility is observed. Nevertheless the subsequent calorimetric structure of peaks cannot be observed in the susceptibility curve which is smoother. The resolution of the magnetic-susceptibility measurement does not allow us to perform a numerical derivative in order to identify some structure. For the case of the polycrystalline sample, heating and cooling measurements of the susceptibility show a very small hysteresis of ~ 2 K. For ferromagnetic materials, magnetic susceptibility is known to depend on field history and thus shows dependence on cycling. This effect is more significant in single-crystalline specimens, par-

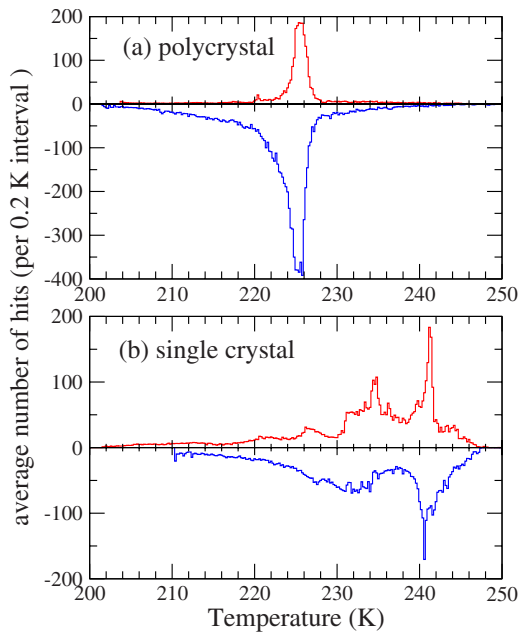


FIG. 2. (Color online) AE activities for (a) the polycrystalline sample and (b) the single crystal for heating and cooling ramps. The activity, on cooling, is shown with a negative sign in order to clarify the picture. Data correspond to an average over 20 ramps performed at 1 K/min.

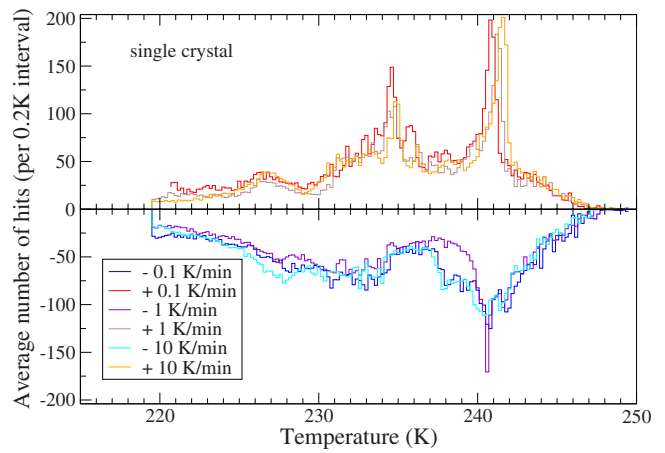


FIG. 3. (Color online) AE activities for the single crystal for heating and cooling ramps at different driving rates, as indicated by the legend. The activity, on cooling, is shown with a negative sign in order to clarify the picture. Data correspond to an average over 20 ramps for 1 and 10 K/min rates and over 10 ramps for the 0.1 K/min rate.

served in the susceptibility curve which is smoother. The resolution of the magnetic-susceptibility measurement does not allow us to perform a numerical derivative in order to identify some structure. For the case of the polycrystalline sample, heating and cooling measurements of the susceptibility show a very small hysteresis of ~ 2 K. For ferromagnetic materials, magnetic susceptibility is known to depend on field history and thus shows dependence on cycling. This effect is more significant in single-crystalline specimens, par-

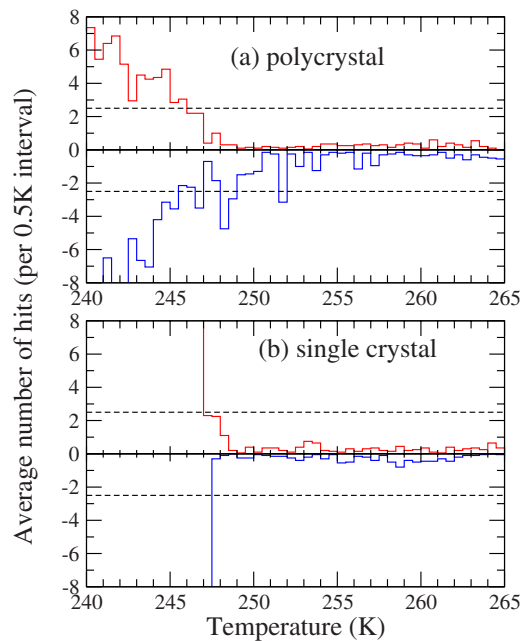


FIG. 4. (Color online) Details of the AE activities for (a) the polycrystalline sample and (b) the single crystal for heating and cooling ramps. The activity, on cooling, is shown as negative in order to clarify the picture. Data correspond to an average over 20 ramps performed at 1 K/min. Note that the bin width is 0.5 K. Dashed lines indicate the noise threshold.

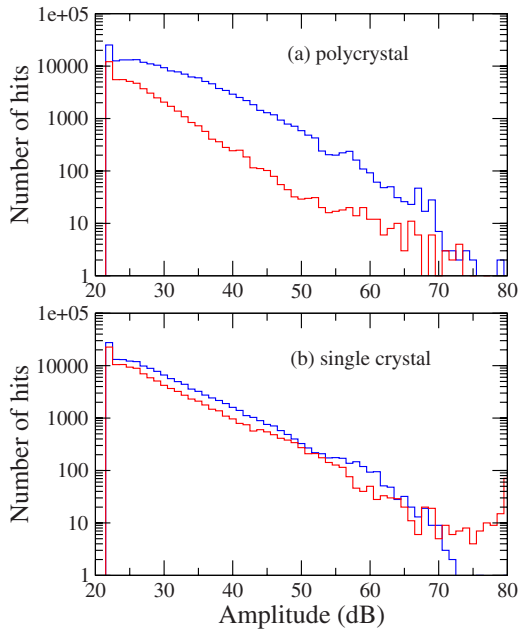


FIG. 5. (Color online) Amplitude distributions for (a) the polycrystal and (b) the single crystal. Blue lines (above) correspond to cooling ramps and red lines (below) to heating ramps. Data have been cumulated over 20 ramps. The cooling or heating rate is 1 K/min. Bin width is 1 dB.

ticularly when a structural transition takes place. This is the reason why cooling and heating runs for the single crystal [Fig. 1(b)] do not match at low temperature. Therefore no reliable data on hysteresis can be obtained in this case.

Figure 2 shows the AE activity as a function of temperature for the single crystal and polycrystal. The first observa-

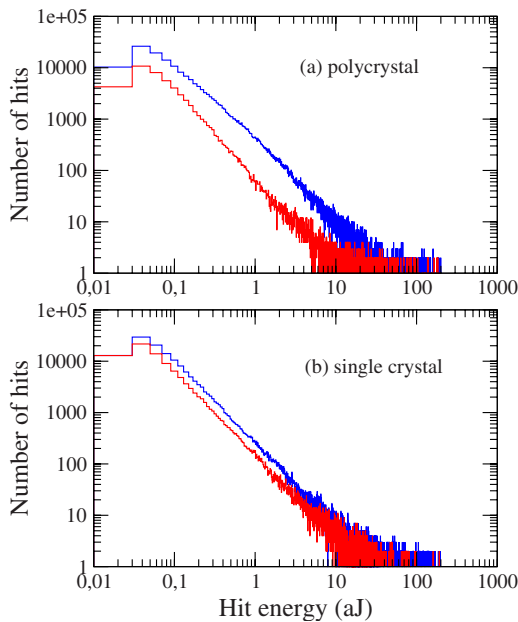


FIG. 6. (Color online) Hit energy distributions for (a) the polycrystal and for (b) the single crystal. Blue (upper) lines correspond to cooling ramps and red (lower) lines to heating ramps. Data have been cumulated over 20 ramps. The cooling and heating rate is 1 K/min. Linear bins have a width of 0.02 aJ.

tion is the strong similarity between the AE activity and the calorimetric curves, as has been reported in many other martensitic transitions.²⁰ Note, nevertheless, that AE activity allows a much better resolution of the details of the transition kinetics.

A second interesting remark, also in agreement with calorimetry, is that the single crystal exhibits a much more structured transition with two to three prominent peaks on cooling and three to four prominent peaks on heating. This peak structure does not depend on the driving rate, as illustrated in Fig. 3. Note that the rate has been changed by 2 orders of magnitude. Although the overlap of the peaks is not as good as the scaling found for other martensitic systems,¹⁷ it indicates that Fe-Pd is very athermal. Also, a similar structure and especially the high peak obtained at the final part of the heating process have been reported from calorimetric measurements in a single crystal of Fe_{70.4}Pd_{29.6} alloy.³ This means that this structure is, to some extent, not a sample-dependent property and that it can be observed in a broad range of compositions.

Note from Fig. 2 that the polycrystal shows a single-peaked and quite smooth transition. This is probably due to the fact that grains exhibit a dispersion of internal strains and boundary conditions that smooth out all the structure that each individual grain may exhibit. An interesting observation is that, although the peak of the activity for the polycrystal (centered around 223 K) seems to be displaced ~ 15 K below the martensitic transition, there are tails of activity that extend clearly many degrees above and below the peak position.

Figure 4 shows details of the AE activity above 240 K. It is important to take into account that the noise threshold, at this rate, is around 2.5 hits/0.5 K interval, indicated by a dashed line in Fig. 4. The first observation is that the beginning of the transition on cooling and the end of the transition on heating are coincident (within ± 2 K) for both the single crystal and the polycrystal. Therefore the differences in the transition temperatures between the polycrystal and the single crystal observed by calorimetry and magnetic-susceptibility measurements are a consequence of the change in the overall profile of the transition kinetic structure, but not of an actual change in the starting temperatures. Some of the grains in the polycrystalline sample start the transformation at the same temperature as the single crystal. Moreover the AE activity also reveals, in agreement with calorimetry and magnetic-susceptibility measurements, that there is almost no hysteresis (within ± 2 K) when looking at the detailed starting and finishing temperatures.

It is also worth noticing the absence of measurable acoustic activity above 250 K. This indicates that if AE associated to pretransitional effects exists, it is below the limit of detectability. Moreover, below the transition, although AE and calorimetry extend for 20–30 K on cooling, the temperature intervals where the nonlinear behavior of the lattice parameters has been reported are much larger. Therefore one can infer that AE is strictly related to the first-order phase transition and occurs all over the coexistence of tetragonal and cubic phases.

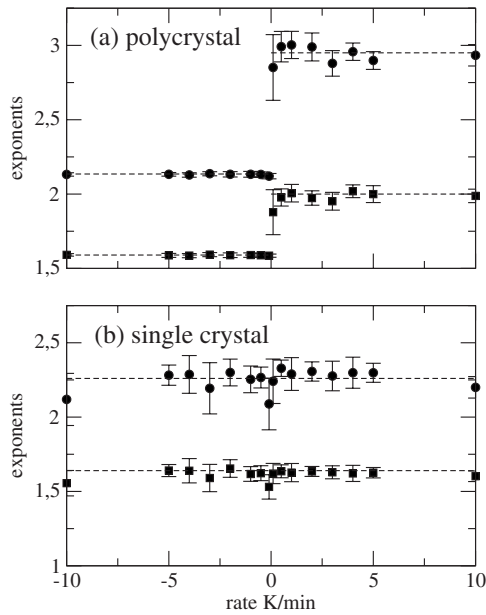


FIG. 7. Fitted exponents for (a) the polycrystal and (b) the single crystal. Circles correspond to the exponent α and squares to ϵ . Dashed lines indicate the values in Table II.

IV. AMPLITUDE AND ENERGY DISTRIBUTIONS

We have studied the amplitude distribution $p(A)$ and energy distribution $p(E)$ for cooling and heating ramps and for different driving rates. In Figs. 5 and 6 we display the histograms corresponding to 1 K/min. Note that the amplitudes in Fig. 5 are measured in decibels and, therefore, the bins used for the histogram are, effectively, logarithmic bins.

The histograms corresponding to the distribution of amplitudes $p(A)$ exhibit an approximate power-law behavior. For the single crystal the behavior extends for more than 2 decades and the slope is approximately the same for cooling and heating ramps. For the polycrystalline sample, the slopes of the histograms differ in the 25–50 dB region (where statistics is high) and a bending of the distribution cannot be disregarded. For the histograms corresponding to energy distribution $p(E)$, the quality of the power-law description is much better and extends for 4 decades for the single crystal and 3 decades for the polycrystal. The polycrystal also exhibits some differences in slope between heating and cooling runs.

The fit of the power-law behavior has been performed by the maximum-likelihood method. The models proposed have

TABLE I. Latent heats and entropy changes obtained from the calorimetric measurements for the samples studied in this paper and for a sample with different composition from the literature.

Sample	ΔH (J/mol)	ΔS (J/K mol)
Single crystal	37	0.164
Polycrystal	20	0.091
Fe _{70.4} Pd _{29.6} (Ref. 3)	88.5	0.30

TABLE II. Exponents α and ϵ obtained from the experimental data by the maximum-likelihood method. The exponent z , which describes the statistical relation between E and A , is calculated from Eq. (4).

Sample	α	ϵ	z
Single crystal	2.26 ± 0.10	1.64 ± 0.10	1.97 ± 0.4
Polycrystal (cooling)	2.135 ± 0.10	1.59 ± 0.10	1.92 ± 0.4
Polycrystal (heating)	2.95 ± 0.10	2.0 ± 0.1	1.95 ± 0.4

a unique free parameter (α or ϵ) and are defined as

$$P(A)dA = \frac{A^{-\alpha}}{Z_A(\alpha)}dA, \quad (1)$$

$$P(E)dE = \frac{E^{-\epsilon}}{Z_E(\epsilon)}dE, \quad (2)$$

where Z_A and Z_E are the normalization factors which are not free in the fit but are functions of the exponents α and ϵ . We have also analyzed the data by considering a two-parameter model that, besides the power-law behavior, includes the exponential prefactors $e^{-\lambda A}$ and $e^{-\lambda E}$. The values of the exponents obtained by these alternative fits are, in all cases, within the error bars of the exponents obtained by the single-parameter model. Therefore, in this work, we give no significance to such exponential corrections.

The fitted exponents as functions of the driving rate are shown in Fig. 7. Data corresponding to cooling ramps are plotted in the negative side of the plot. Each exponent value corresponds to an average over 20 equivalent ramps (except for the 0.1 K/min data that have been averaged over 10 ramps). Moreover, in order to discard aging effects, the ramps corresponding to different rates are not performed sequentially by increasing or decreasing the rate, but randomly ordered.

As can be seen there is no significant dependence of the exponents on the rate. This means that the sample keeps its athermal character for all the studied driving rates. This is in contrast to what has been observed in other MT.^{17,18} Moreover the single crystal shows no dependence of the exponents when comparing heating and cooling ramps, whereas for the polycrystal the difference is clear for both the amplitude and energy exponents. The numerical values of the exponents are summarized in Table II.

The value $\alpha=2.26$ obtained for the single crystal can be compared with the values found for other single-crystalline samples. Some years ago, it was proposed that this exponent is universal and characteristic of all the martensitic transitions with the same symmetry change.¹⁶ Different Cu-based alloys transforming from a cubic structure to a monoclinic one (18R) had $\alpha=3.1 \pm 0.2$ and those transforming from cubic to orthorhombic (2H) had $\alpha=2.4 \pm 0.2$. Later it was realized¹⁸ that the true universal value is only obtained when the thermal driving of the sample is adiabatic. This has two implications: on one hand, the rate should be slow enough to prevent overlap of the signals corresponding to independent transformation events.²¹ On the other hand, for systems

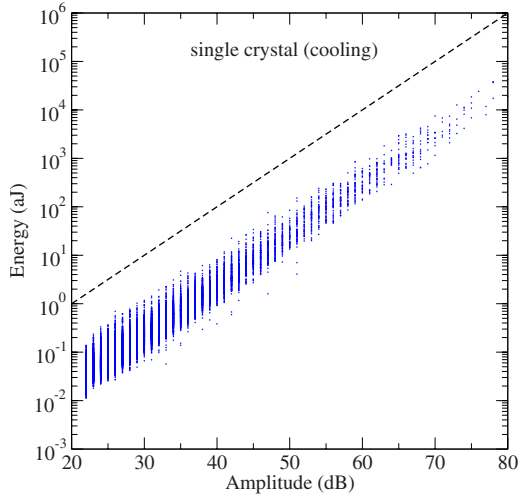


FIG. 8. (Color online) Hit energy versus hit amplitude cloud maps corresponding to cooling ramps of the single crystal. Data have been averaged over 20 ramps. The cooling and heating rate is 1 K/min. The dashed line indicates the behavior $E \sim A^2$.

which do not behave athermally, the driving should be fast enough to prevent nucleation due to thermal fluctuations. This last point suggests that the value proposed for the transformation from cubic to orthorhombic should be higher than $\alpha = 2.4 \pm 0.2$. In our case corresponding to a transition from cubic to tetragonal symmetry, the independence of the exponent with the driving rate (when changing it by 2 orders of magnitude) is good evidence that the system is athermal and that the exponent is close to the adiabatic one.

The values of α and ϵ obtained suggest that there is a generic statistical dependence $E \sim A^z$. Indeed, by proposing such a change of variables in the power-law probability density $p(E)$ [from Eq. (2)], we get

$$p(E)dE \sim E^{-\epsilon}dE \sim A^{-\epsilon}A^{z-1}dA. \quad (3)$$

By comparing with Eq. (1), we deduce that

$$z = \frac{\alpha - 1}{\epsilon - 1}. \quad (4)$$

One gets, therefore, the exponents indicated in Table I, totally compatible with a dependence $E \sim A^2$. This dependence can be directly checked from the experimental data by plotting a cloud map of E versus A . An example corresponding to the single crystal (cooling ramps) is shown in Fig. 8. Similar plots for the heating ramps and for the polycrystal give the same good agreement.

We note that this dependence is in contradiction with some hypotheses which have been proposed in the context of theoretical models for the study of criticality associated to noise in disordered systems²² and in the context of Barkhausen noise.^{23,24} According to these works, criticality implies that the average pulse shape will scale in a universal way. Thus a pulse with amplitude A and duration Δt should be described by

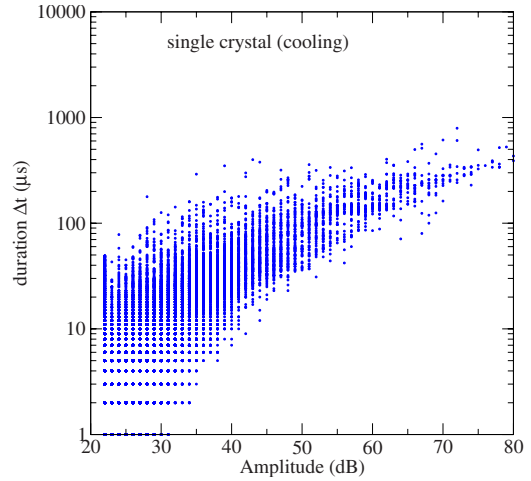


FIG. 9. (Color online) Hit duration versus hit amplitude cloud maps corresponding to cooling ramps of the single crystal. Data have been averaged over 20 ramps. The cooling and heating rate is 1 K/min.

$$V_{A,\Delta t}(t) = A\Phi(t/\Delta t), \quad (5)$$

where Φ is a universal function. Together with this hypothesis it is assumed that there is a statistical scaling relation between amplitudes and durations, $A \sim \Delta t^x$ (the exponent x is called $1/\sigma\nu z - 1$ in Refs. 22–24). Combining these two hypotheses, one can compute the energy by integration of the square of the signal $V_{A,\Delta t}(t)$ as

$$E \propto \int_0^{\Delta t} A^2\Phi^2(t/\Delta t)dt \propto A^2\Delta t \propto A^{2+1/x}. \quad (6)$$

Our $z=2$ value is not compatible with any reasonable value of the exponent x . On the other hand, one can directly test the $A \sim \Delta t^x$ behavior from the experimental data by plotting cloud maps of amplitude A vs durations Δt . An example corresponding to 20 cooling ramps for the single crystal is shown in Fig. 9. The plots for the polycrystal and the heating ramps give similar results.

As can be seen the cloud exhibits a bend for large amplitudes incompatible with the hypothesis $A \sim \Delta t^x$. Such a dependence $A \sim \Delta t^x$ with $x \approx 1$ was also proposed some time ago from AE studies of martensitic transitions in Cu-based alloys,^{8,10} on the basis of plots very similar to that in Fig. 9, although the poorer quality of the statistics did not allow us to distinguish the bend in the large- A region.

V. SUMMARY AND CONCLUSION

We have studied the AE in two samples of $\text{Fe}_{68.8}\text{Pd}_{31.2}$, a single crystal and a polycrystal, as a function of temperature in the range of 200–265 K. Our study has revealed that significant AE activity only occurs during the first-order martensitic transition from a fcc to a fct structure. We have not detected AE associated with premartensitic phenomena nor with the low-temperature lattice-parameter changes reported in the literature.⁵ The accurate measurement of AE activity above the noise threshold has revealed that for the two

samples the transition starts at the same temperature on cooling and ends at the same transition on heating (± 2 K). Moreover we have found, in agreement with calorimetry and magnetic-susceptibility measurements, that if there is any hysteresis, it is smaller than ± 2 K.

The transition in the single-crystal sample proceeds by a complex kinetic structure, characterized by several peaks of activity extending for more than 35 K. This structure is very similar to the one observed by calorimetric measurements and independent of the heating and cooling rate, which reflects the athermal character of the transition. For the polycrystal the transition is smoother, also in agreement with calorimetry, and displays a single peak whose maximum is located 20 K below the transition starting temperature.

The statistical analysis of the AE individual events (hits) has shown that for the single crystal the amplitude and energy distributions are power laws, characterized by the exponents $\alpha=2.26 \pm 0.1$ and $\epsilon=1.64 \pm 0.1$, respectively. The exponents are the same for heating and cooling ramps and are also independent of the driving rate. For the polycrystal the power-law behavior of the distributions is not so well defined and the fitted exponents are independent of the rate but dif-

ferent when comparing heating and cooling ramps. In the two cases, the fitted exponents are compatible with a statistical relation $E \sim A^2$.

Finally we have discussed the results corresponding to the single crystal in comparison with some recent theories²²⁻²⁴ that propose the scaling of the shape of the individual pulses. We have shown that the relation $E \sim A^2$ and the assumption that the signal amplitude should be statistically related to the signal duration by $A \sim \Delta t^x$ are not compatible with current scaling hypotheses.

ACKNOWLEDGMENTS

The authors thank Uwe Klemradt for providing his laboratories and the acoustic emission setup that was used for part of the experiments. This work received financial support from CICyT (Spain), under Project No. MAT2007-61200; CIRIT (Catalonia), under Project No. 2005SGR00969; EU (Marie Curie RTN MULTIMAT), under Contract No. MRTN-CT-2004-5052226; JSPS (Japan), under Grant No. Kiban B18360331; and MEXT, Japan, Global COE (B11).

¹C. B. Scruby, J. Phys. E **20**, 946 (1987).

²T. Ichitsubo, K. Tanaka, M. Koiwa, and Y. Yamazaki, Phys. Rev. B **62**, 5435 (2000).

³J. Cui, T. W. Shield, and R. D. James, Acta Mater. **52**, 35 (2004).

⁴M. Mitsuka, T. Ohba, T. Fukuda, T. Kakeshita, and M. Tanaka, Mater. Sci. Eng., A **438-440**, 332 (2006).

⁵T. Kakeshita, T. Fukuda, and T. Takeuchi, Mater. Sci. Eng., A **438-440**, 12 (2006).

⁶S. Muto, S. Takeda, R. Oshima, and F. E. Fujita, J. Phys.: Condens. Matter **1**, 9971 (1989).

⁷H. Seto, Y. Noda, and Y. Yamada, J. Phys. Soc. Jpn. **59**, 978 (1990).

⁸E. Vives, I. Ràfols, Ll. Mañosa, J. Ortín, and A. Planes, Phys. Rev. B **52**, 12644 (1995).

⁹E. Vives, J. Ortín, L. Mañosa, I. Ràfols, R. Pérez-Magrané, and A. Planes, Phys. Rev. Lett. **72**, 1694 (1994).

¹⁰I. Ràfols and E. Vives, Phys. Rev. B **52**, 12651 (1995).

¹¹L. Straka, V. Novak, M. Landa, and O. Heczko, Mater. Sci. Eng., A **374**, 263 (2004).

¹²F. J. Pérez-Reche, E. Vives, L. Mañosa, and A. Planes, Mater. Sci. Eng., A **378**, 353 (2004).

¹³V. A. Plotnikov, J. Phys. IV **112**, 701 (2003).

¹⁴Z. Yu and P. C. Clapp, J. Appl. Phys. **62**, 2212 (1987).

¹⁵S. M. C. VanBohemen, M. J. M. Hermans, and G. Ouden, Mat. Sci. Technol. **18**, 1524 (2002).

¹⁶Ll. Carrillo, Ll. Mañosa, J. Ortín, A. Planes, and E. Vives, Phys. Rev. Lett. **81**, 1889 (1998).

¹⁷F. J. Pérez-Reche, E. Vives, L. Mañosa, and A. Planes, Phys. Rev. Lett. **87**, 195701 (2001).

¹⁸F. J. Pérez-Reche, B. Tadic, L. Mañosa, A. Planes, and E. Vives, Phys. Rev. Lett. **93**, 195701 (2004).

¹⁹M. L. Goldstein, S. A. Morris, and G. G. Yen, Eur. Phys. J. B **41**, 255 (2004).

²⁰A. Planes, J. L. Macqueron, M. Morin, and G. Guénin, Phys. Status Solidi A **66**, 717 (1981).

²¹R. A. White and K. A. Dahmen, Phys. Rev. Lett. **91**, 085702 (2003).

²²M. C. Kuntz and J. P. Sethna, Phys. Rev. B **62**, 11699 (2000).

²³A. P. Mehta, A. C. Mills, K. A. Dahmen, and J. P. Sethna, Phys. Rev. E **65**, 046139 (2002).

²⁴F. Colaiori, S. Zapperi, and G. Durin, J. Magn. Magn. Mater. **272-276**, e533 (2004).